Further Results on Plant Parameter Identification using Continuous-Time Multiple-Model Adaptive Estimators

Vahid Hassani, A. Pedro Aguiar, António M. Pascoal and Michael Athans

***Abstract*— This paper describes a deterministic approach to adaptive state and parameter estimation using a multiple model structure. In the set-up adopted, the plant of interest is described by a finite dimensional model with parametric uncertainty. To each choice of a finite number of parameter values there corresponds a finite set of multiple design models and a corresponding set of observers. Assuming the latter have been chosen, a Dynamic Weighting Signal Generator (DWSG) performs on-line adaptation of the weights given to the individual observer estimates based on the energy of the output error signals. In the present paper we develop a distance-like pseudo norm between the true plant and the identified model in a deterministic setting, based on the energy of the output error signals. Furthermore we show, under a distinguishability condition, that the model identified is the one that is closest to the true plant in the defined deterministic norm. We also prove that the convergence of the parameter estimate is exponentially fast. Performance and convergence of the CT-MMAE procedure are illustrated with Monte-Carlo simulation runs using the model of an inverted pendulum.**

I. Introduction

In many practical applications of estimation theory, it is virtually impossible to obtain a highly accurate mathematical model of the physical process of interest. For this reason, a model is often given in terms of its basic structure and a vector of parameters in a compact set that capture plant parameter uncertainty. When state estimation for this type of systems is carried out, the variations of the parameters and their identification play a critical role. Also, it is often necessary to estimate both a system's parameter vector and its state.

Many approaches have been proposed to perform state estimation together with parameter identification. There is one class of adaptive estimation scheme which calls for the construction of a bank of local estimators, where each estimator is matched to a possible parameter value [1]–[8]. The optimal state estimate is obtained via a weighted sum over the local estimates, together with the dynamics of the weighting factors. Based upon this idea, algorithms for both adaptive estimation and control have been designed. The resulting estimators, usually referred to as Multiple Model Adaptive Estimators (MMAE), are easy to implement and exhibit a parallel structure. In this approach, a set of models (estimators) is designed to cover the possible system behavior "patterns" or structures and the overall estimated output is obtained by adequate combination of the local estimated outputs based on each individual model.

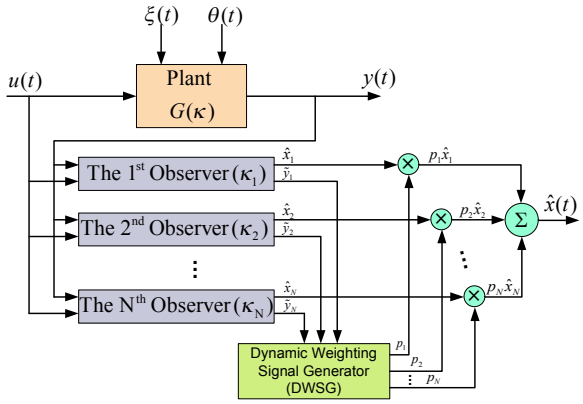

Fig. 1. The CT-MMAE architecture

In the standard version of MMAE [1]–[3] a separate discrete-time Kalman filter (KF) is developed based on each different assumed value of the uncertain parameter defining a "model". The resulting set of KFs forms a "model-set" where each local KF generates its own state estimate and an output error (residual) as shown in Fig. 1. All the KFs in the model-set run in parallel and at each sample time the residuals are used to compute, for the i^{th} KF, the conditional probability p_i that it corresponds to the correct parameter value. The overall state estimate is a probabilistically weighted combination of each KF's estimate.

In [3], discrete time MMAE structures were analyzed by introducing an information theoretic measure. In particular, the authors studied the convergence of the conditional probabilities p_i and showed that the one corresponding to the KF designed for the closest to the actual system (in a stochastic norm sense) converges to one, while the others tend to zero. However, the theoretical setup exploited in [3] requires extensive knowledge of stochastic analysis, information theory, and measure theory.

Notwithstanding the numerous works on discrete-time MMAE, not many results are available for Continuous-Time MMAE. The stochastic continuous-time MMAE (CT-MMAE) was introduced in [9] and [10] but no further research has been carried out on this subject, to the best of our knowledge (except [6], [7]). In this case, the dynamic weights are generated by a continuous time differential equation. No convergence results were derived in [9], [10]. In [7],

This work was supported in part by project GREX / CEC-IST (Contract No. 035223), the FREESUBNET RTN of the CEC, Co3-AUVs (EU FP7 under grant agreement No. 231387), DENO / FCT-PT (PTDC/EEA-ACR/67020/2006), and the FCT-ISR/IST plurianual funding program (through the POS C initiative in cooperation with FEDER). The first author benefited from a PhD grant from the Foundation for Science and Technology (FCT), Portugal.

The authors are with the Institute for Systems and Robotics (ISR), Instituto Superior Técnico (IST), Lisbon, Portugal. Tel: (+351) 21 841 8054, Fax: (+351) 21 841 8291 {vahid,pedro,antonio,athans}@isr.ist.utl.pt

Michael Athans is also Professor of EECS (emeritus), M.I.T., USA.

a different method for generating the dynamic weights was used and the convergence of dynamic weights was proved under a very tight distinguishability condition.

Here we show for the first time that the key results obtained in [3] in a stochastic, discrete-time setting, can be extended to continuous-time by resorting to a much simpler deterministic framework that relies on the use of Krener Observers (KO) [11] rather than Kalman Filters. We show, under a suitable distinguishability condition, that the model identified is the one that is the closest to the true plant among the bank of observers in a defined deterministic norm. The distinguishability condition that we use is weaker than the one in [7] and the convergence proof is far simpler.

The structure of the paper is as follows. In section II we review the main issues of CT-MMAE and define the structure of a CT-MMAE consisting of a finite number of observers and a Dynamic Weighting Signal Generator (DWSG). Section III summarizes our main results. Section IV illustrates the performance of the CT-MMAE algorithm proposed, through computer simulations with a model of an inverted pendulum. Conclusions and suggestions for future research are summarized in Section V.

II. The Continuous-Time Multiple-Model Adaptive Estimator

In this section we describe a class of CT-MMAE using a deterministic setting. The MMAE relies on a finite number N of selected models (SMs) chosen from the original set of (possibly infinite) plant models and consists of: i) a dynamic generator of N weighting signals and ii) a bank of N continuous-time observers, where each observer is designed based on one of the SMs adopted. The state estimate is generated by a weighted sum of the local state-estimates produced by the bank of observers. The dynamic weights are generated by a differential dynamic equation called Dynamic Weighting Signal Generator (DWSG). Fig. 1 shows the structure of the CT-MMAE in which the plant is described by an LTI differential equation, $\xi(t)$ and $\theta(t)$ are deterministic plant and measurement noise respectively, and the observers are designed using different values of the uncertain parameters.

We assume the plant model G is subjected to parameter uncertainty $\kappa \in \mathbb{R}^l$, that is, $G = G(\kappa)$. In what follows we consider multiple-input-multiple-output (MIMO) linear plant models of the form

$$\dot{x}(t) = A_\kappa(t)x(t) + B_\kappa(t)u(t) + G_\kappa(t)\xi(t), \quad (1a)$$
$$y(t) = C_\kappa(t)x(t) + \theta(t), \quad (1b)$$

where $x(t) \in \mathbb{R}^n$ denotes the state of the system, $u(t) \in \mathbb{R}^m$ its control input, $y(t) \in \mathbb{R}^q$ its measured noisy output, $\xi(t) \in \mathbb{R}^r$ an input plant disturbance that cannot be measured, and $\theta(t) \in \mathbb{R}^q$ is the measurement noise. The initial condition $x(0)$ of (1) and the signals $\xi(t)$ and $\theta(t)$ are assumed unknown but bounded. The matrices A_κ, B_κ, L_κ, and C_κ contain *unknown constant parameters* denoted by vector κ. Consider a finite set of candidate parameter values $\boldsymbol{\kappa} := \{\kappa_1, \kappa_2, \ldots, \kappa_N\}$ indexed by $i \in \{1, \ldots, N\}$. We recall the following CT-MMAE structure. The state estimate is given by

$$\hat{x}(t) := \sum_{i=1}^{N} p_i(t)\hat{x}_i(t), \quad (2)$$
$$\hat{y}(t) := \sum_{i=1}^{N} p_i(t)\hat{y}_i(t), \quad (3)$$
$$\hat{\kappa}(t) := \kappa_{i^\star}, \quad i^\star := \arg \max_{i \in \{1,\ldots,N\}} p_i(t), \quad (4)$$

where $\hat{x}(t)$, $\hat{y}(t)$ and $\hat{\kappa}(t)$ are the estimates of the state $x(t)$, output $y(t)$, and parameter vector κ at time t, respectively and $p_i(t)$ are dynamic weights (which are defined below). In (2), each $\hat{x}_i(t)$; $i = 1, \ldots, N$ corresponds to a "local" state estimate generated by the i^{th} observer which is a Krener minmax observer [11] of the type[1]

$$\dot{P}_i = A_{\kappa_i}P_i + P_iA_{\kappa_i}^T + G_{\kappa_i}\Xi G_{\kappa_i}^T - P_iC_{\kappa_i}^T\Theta^{-1}C_{\kappa_i}P_i, \quad (5a)$$
$$\dot{\hat{x}}_i = A_{\kappa_i}\hat{x}_i + B_{\kappa_i}u + H_{\kappa_i}\big(y - C_{\kappa_i}\hat{x}_i\big), \quad (5b)$$
$$\hat{y}_i = C_{\kappa_i}\hat{x}_i, \quad (5c)$$

where $[A_{\kappa_i}, G_{\kappa_i}]$ and $[A_{\kappa_i}, C_{\kappa_i}]$ are assumed to be controllable and observable, respectively for $i = 1, \ldots, N$ and the symmetric positive definite weighting matrices Ξ and Θ are viewed as tuning parameters that can be chosen based on the information available about the plant model as well as the disturbance and measurement noise acting on it. Furthermore, $H_{\kappa_i} = P_iC_{\kappa_i}^T\Theta^{-1}$.

In the sequel we introduce dynamic weights which weigh the local estimations (2) and determine the estimation of the uncertain parameter (4).

A. Dynamic Weighting Signal Generator (DWSG)

In the proposed CT-MMAE, the dynamic weights $p_i(t) \in \mathbb{R}$, $i = 1, \ldots, N$ satisfy

$$\dot{p}_i(t) = -\lambda\Big(1 - \frac{\beta_i(t)e^{-\omega_i(t)}}{\sum_{j=1}^{N} p_j(t)\beta_j(t)e^{-\omega_j(t)}}\Big)p_i(t), \quad (6)$$

where λ is a positive constant, $\beta_i(t)$ is a signal assumed to satisfy the condition $c_1 \leq \beta_i(t) \leq c_2$ for some positive constants c_1, c_2, and $\omega_i(\cdot)$ is a continuous function called an *error measuring function* that maps the measurable signals of the plant and the states of the i^{th} local estimator to a nonnegative real value. An example of an error measuring function and a $\beta_i(t)$ function, which used throughout this paper, are $\omega_i(t) := \frac{1}{2}\|\hat{y}_i(t) - y(t)\|^2_{S_i^{-1}(t)}$ and $\beta_i(t) := \frac{1}{\sqrt{\det S_i(t)}}$, respectively, where $S_i(t)$ is a uniformly bounded positive definite weighted matrix and $\|x\|_S = \big(x^TSx\big)^{\frac{1}{2}}$. The matrices S_{κ_i} are important to scale the energy of estimation error signals in order to make them comparable. In what follows, we name equation (6) as the dynamic weighting signal generator (DWSG). The structure of the DWSG, which generates the time-evolution of the weights $p_i(t)$, is introduced in [7].

We impose the constraint that the initial conditions $p_i(0)$ be chosen such that $p_i(0) \in (0, 1)$ and $\sum_{i=1}^{N} p_i(0) = 1$.

[1]For simplicity of notation, we will drop the time index notation.

The parameters Ξ, Θ and the functions β_i, w_i are tuning parameters/functions of the CT-MMAE chosen by the designer based on the system being modeled.

III. Convergence Results

In this section we summarize our main results regarding the CT-MMAE. Positiveness and boundedness of the dynamic weights $p_i(t)$, generated by (6) were shown in [7] to be independent of the input signals of the dynamic weighting signal generator (DWSG) system. It was further shown that the sum of the p_i's is always one for all $t \geq 0$ (see Theorem 1 in [7] for more details).

We next provide conditions for convergence of the dynamic weights $p_i(t)$.

Theorem 1: Let $i^\star \in \{1, 2, \ldots, N\}$ be an index of a parameter vector in κ and $\mathcal{I} := \{1, 2, \ldots, N\} \backslash i^\star$ an index set. Suppose that there exists a positive constant T such that for all $t \geq 0$ and all $j \in \mathcal{I}$ the following condition holds:

$$\frac{1}{T}\int_t^{t+T} \big(\omega_{i^\star}(\tau) - \ln \beta_{i^\star}(\tau)\big)\, d\tau < \frac{1}{T}\int_t^{t+T} \big(w_j(\tau) - \ln \beta_j(\tau)\big)\, d\tau. \quad (7)$$

Then, $p_{i^\star}(t)$ governed by (6) satisfies

$$\lim_{t\to\infty} p_{i^\star}(t) = 1. \quad (8)$$

Conversely, if (8) is observed, then there exist positive constants T such that for all $t \geq 0$ and all $j \in \mathcal{I}$

$$\frac{1}{T}\int_t^{t+T} \big(\omega_{i^\star}(\tau) - \ln \beta_{i^\star}(\tau)\big)\, d\tau \leq \frac{1}{T}\int_t^{t+T} \big(w_j(\tau) - \ln \beta_j(\tau)\big)\, d\tau.^2 \quad (9)$$

□

Proof: From (6) we obtain for each $i \in \{1, 2, \ldots, N\}$

$$p_i(t) = p_i(0) \exp\Big(\int_0^t \psi_i(\tau)\, d\tau\Big), \quad (10)$$

where $\psi_i(t) := -\lambda\big(1 - \frac{\beta_i(t)e^{-\omega_i(t)}}{\sum_{j=1}^N p_j\beta_j(t)e^{-\omega_j(t)}}\big)$.
Define

$$L_j(t) := \frac{p_j(t)}{p_{i^\star}(t)}; \quad j \in \mathcal{I}. \quad (11)$$

Using (10) we obtain

$$L_j(t) = \frac{p_j(0)}{p_{i^\star}(0)} \frac{e^{\int_0^t \lambda \frac{\beta_j(\tau)e^{-w_j(\tau)} - \sum_{j=1}^N p_j(\tau)\beta_j(\tau)e^{-w_j(\tau)}}{\sum_{j=1}^N p_j(\tau)\beta_j(\tau)e^{-w_j(\tau)}} d\tau}}{e^{\int_0^t \lambda \frac{\beta_{i^\star}(\tau)e^{-w_{i^\star}(\tau)} - \sum_{j=1}^N p_j(\tau)\beta_j(\tau)e^{-w_j(\tau)}}{\sum_{j=1}^N p_j(\tau)\beta_j(\tau)e^{-w_j(\tau)}} d\tau}}, \quad (12)$$

[2]Note that in (9) the inequality is not strict.

and therefore it follows that

$$L_j(t+T) = \frac{e^{\int_t^{t+T} \lambda \frac{\beta_j(\tau)e^{-w_j(\tau)} - \sum_{j=1}^N p_j(\tau)\beta_j(\tau)e^{-w_j(\tau)}}{\sum_{j=1}^N p_j(\tau)\beta_j(\tau)e^{-w_j(\tau)}} d\tau}}{e^{\int_t^{t+T} \lambda \frac{\beta_{i^\star}(\tau)e^{-w_{i^\star}(\tau)} - \sum_{j=1}^N p_j(\tau)\beta_j(\tau)e^{-w_j(\tau)}}{\sum_{j=1}^N p_j(\tau)\beta_j(\tau)e^{-w_j(\tau)}} d\tau}} L_j(t). \quad (13)$$

Taking logarithms of both sides,

$$\begin{aligned}
&\ln \frac{L_j(t+T)}{L_j(t)} \\
&= \int_t^{t+T} \lambda \frac{\beta_j(\tau)e^{-w_j(\tau)} - \sum_{j=1}^N p_j(\tau)\beta_j(\tau)e^{-w_j(\tau)}}{\sum_{j=1}^N p_j(\tau)\beta_j(\tau)e^{-w_j(\tau)}} d\tau \\
&- \int_t^{t+T} \lambda \frac{\beta_{i^\star}(\tau)e^{-w_{i^\star}(\tau)} - \sum_{j=1}^N p_j(\tau)\beta_j(\tau)e^{-w_j(\tau)}}{\sum_{j=1}^N p_j(\tau)\beta_j(\tau)e^{-w_j(\tau)}} d\tau \\
&= \int_t^{t+T} \lambda \frac{\beta_j(\tau)e^{-w_j(\tau)} - \beta_{i^\star}(\tau)e^{-w_{i^\star}(\tau)}}{\sum_{j=1}^N p_j(\tau)\beta_j(\tau)e^{-w_j(\tau)}} d\tau. \quad (14)
\end{aligned}$$

Applying condition (7), we can conclude that there exists $\delta > 0$ such that

$$\frac{1}{T}\int_t^{t+T} \big(-w_{i^\star}(\tau) + \ln \beta_{i^\star}(\tau)\big)\, d\tau - \delta/2 > \frac{1}{T}\int_t^{t+T} \big(-w_j(\tau) + \ln \beta_j(\tau)\big)\, d\tau + \delta/2.$$

Because $\exp(\cdot)$ is a monotonically increasing function we can conclude that

$$\Big(\frac{1}{T}\int_t^{t+T} \beta_{i^\star}(\tau)e^{-w_{i^\star}(\tau)}\, d\tau\Big)e^{-\delta/2} > \Big(\frac{1}{T}\int_t^{t+T} \beta_j(\tau)e^{-w_j(\tau)}\, d\tau\Big)e^{\delta/2}$$

holds. Therefore, there exists $\varepsilon > 0$ such that

$$\frac{1}{T}\int_t^{t+T} \beta_{i^\star}(\tau)e^{-w_{i^\star}(\tau)} d\tau - \frac{1}{T}\int_t^{t+T} \beta_j(\tau)e^{-w_j(\tau)} d\tau > \varepsilon,$$

and therefore

$$\int_t^{t+T} \beta_{i^\star}(\tau)e^{-w_{i^\star}(\tau)} - \beta_j(\tau)e^{-w_j(\tau)} d\tau > T\varepsilon.$$

Denoting $\underline{w} := \inf_{t\geq 0}\big(\min_{j\in\mathcal{I}} w_j(t)\big)$ and $\overline{\beta} := \sup_{t\geq 0}\big(\max_{j\in\mathcal{I}} \beta_j(t)\big)$, and using the fact that $\sum_{j=1}^N p_j(t)\beta_j(t)e^{-w_j(t)} > 0$ we can conclude that

$$\int_t^{t+T} \frac{\beta_{i^\star}(\tau)e^{-w_{i^\star}(\tau)} - \beta_j(\tau)e^{-w_j(\tau)}}{\sum_{j=1}^N p_j(\tau)\beta_j(\tau)e^{-w_j(\tau)}} d\tau \geq \int_t^{t+T} \frac{\beta_{i^\star}(\tau)e^{-w_{i^\star}(\tau)} - \beta_j(\tau)e^{-w_j(\tau)}}{\overline{\beta}e^{-\underline{w}}} d\tau > T\varepsilon_1, \quad (15)$$

where $\varepsilon_1 = \frac{\varepsilon}{\overline{\beta}e^{-\underline{w}}} > 0$.

Combining (15) with (14), we further conclude that

$$\ln \frac{L_j(t+T)}{L_j(t)} \; < \; -T\lambda\varepsilon_1 \tag{16}$$

or, equivalently,

$$L_j(t+T) \; < \; e^{\left(-T\lambda\varepsilon_1\right)} \, L_j(t). \tag{17}$$

It follows that $L_j(t) = \frac{p_j(t)}{p_{i^\star}(t)}$ converges to zero for all $j \in \mathcal{I}$, as $T \to \infty$. Since $\sum_{j=1}^{N} p_j(0) = 1$, it is now straightforward to conclude that $p_j(t) \to 0$, and $p_{i^\star}(t) \to 1$. Furthermore, the convergence is exponentially fast.

To prove that (8) implies (9), suppose that (8) holds but (9) does not. Then

$$\frac{1}{T}\int_t^{t+T} \left(\omega_{i^\star}(\tau) - \ln \beta_{i^\star}(\tau)\right) d\tau \\ > \frac{1}{T}\int_t^{t+T} \left(w_j(\tau) - \ln \beta_j(\tau)\right) d\tau, \tag{18}$$

and by following the same steps as above, we can conclude that $p_j(t) \to 1$ as $t \to \infty$, implying $p_{i^\star}(t) \to 0$ as $t \to \infty$, which contradicts (8). Thus, (8) implies (9).

■

Condition (7) can be viewed as a "*distinguishability*" criterion and implies that for sufficiently large T one of the local observers will exhibit less output error (residual) "energy". In fact, based on the result of Theorem 1 the following Corollary holds for Linear Time-Invariant (LTI) systems using weighted quadratic norms of the output estimation errors for the error measuring functions.

Corollary 1: [Corollary 4 in [7]] Suppose that the conditions of Theorem 1 hold and let the input signal $\eta = [\xi(t)\ \theta(t)\ u(t)]^T$ be a bounded-spectral signal with power spectral density $\Psi_\eta(\omega)$. Further, let $w_i(t) := \frac{1}{2}\|y(t) - \hat{y}_i(t)\|^2_{S_i^{-1}}$. Then, the parameter estimate $\hat{\kappa}_t$ converges to the closest to the true parameter κ as $t \to \infty$, in the following sense:

$$\lim_{t\to\infty} \hat{\kappa}_t = \kappa_{i^\star}, \tag{19a}$$

$$i^\star = \arg \min_{i\in\{1,\ldots,N\}} \{\Upsilon_{\kappa_1,\kappa}, \Upsilon_{\kappa_2,\kappa}, \ldots, \Upsilon_{\kappa_N,\kappa}\} \tag{19b}$$

$$\Upsilon_{\kappa_i,\kappa} = tr[\frac{1}{2\pi}\int_{-\infty}^{\infty} (\mathbb{H}_i(j\omega)\Psi_\eta(\omega)\mathbb{H}_i(j\omega)^H S_{\kappa_i}^{-1})\, d\omega] - \ln \beta_i \tag{19c}$$

where $\mathbb{H}_i(s)$ is the transfer matrix function defined by

$$\mathbb{H}_i(s) = \mathbb{C}_i(sI - \mathbb{A}_i)^{-1}\mathbb{B}_i + \mathbb{D}, \tag{20}$$

with

$$\mathbb{A}_i := \begin{bmatrix} A_\kappa & 0 \\ H_{\kappa_i}C_\kappa & A_{\kappa_i} - H_{\kappa_i}C_{\kappa_i} \end{bmatrix}, \quad \mathbb{C}_i := \begin{bmatrix} C_\kappa & -C_{\kappa_i} \end{bmatrix},$$
$$\mathbb{B}_i := \begin{bmatrix} G_\kappa & 0 & B_\kappa \\ 0 & H_{\kappa_i} & B_{\kappa_i} \end{bmatrix}, \qquad \mathbb{D} := \begin{bmatrix} 0 & I & 0 \end{bmatrix}.$$

□

For the proof of Corollary 1, the reader is referred to [7], [8], [12].

Based on the results of Corollary 1 we can define a deterministic norm on the set of stable plants given by

$$d(\kappa_i;\kappa_j) := |\Upsilon_{\kappa_i,\kappa^\star} \; - \; \Upsilon_{\kappa_j,\kappa^\star}|. \tag{21}$$

Theorem 2: The deterministic norm in (21) is a Pseudo Norm. □

Proof: A proof is available in [12]. ■

We now show that the convergence results derived in Theorem 1 are also valid if the aforementioned norm d is used instead of $\Upsilon_{\kappa_i,\kappa^\star}$.

Corollary 2:

$$d(\kappa_i;\kappa^\star) \geq d(\kappa_j;\kappa^\star)$$

if and only if

$$\Upsilon_{\kappa_i,\kappa^\star} \geq \Upsilon_{\kappa_j,\kappa^\star}.$$

□

Proof: A proof is available in [12]. ■

IV. Illustrative Example

The CT-MMAE procedure is now evaluated through an example of an inverted pendulum (also known as cart and pole system) which consists of a thin rod attached at its bottom to a moving cart connected to a wall with a known spring (depicted in Fig. 2).

The output signals are the position of the cart $x(t)$ (in meters) and the angle of the the pendulum $\theta(t)$ (in radians) corrupted by independent zero mean white noise with intensity of 10^{-7} and 10^{-8}, respectively.

The measuring functions $w_i(t) = \frac{1}{2}(y(t) - \hat{y}_i(t))^T S_i^{-1}(y(t) - \hat{y}_i(t))$ were used during the simulations. A state-space representation of the plant, including the disturbance and noise inputs, is given by

$$\dot{x}(t) = A\,x(t) + B\,u(t) + G\,\xi(t),$$
$$y(t) = Cx(t) + \theta(t),$$

where $u(t)$ is the control force (N), $w(t)$ is the disturbance force (N) affecting the cart, $v(t)$ is measurement noise, and the state vector is $[x\ \theta\ \dot{x}\ \dot{\theta}]^T$. The system matrices (A, B, C) are given by

$$A = \begin{bmatrix} 0 & 0 & 1 & 0 \\ 0 & 0 & 0 & 1 \\ -\frac{k}{M} & -\frac{mg}{M} & -\frac{b}{M} & 0 \\ \frac{k}{LM} & \frac{m+M}{LM}g & \frac{b}{LM} & 0 \end{bmatrix}, \; B = \begin{bmatrix} 0 \\ 0 \\ \frac{1}{M} \\ -\frac{1}{LM} \end{bmatrix}, \quad G = \begin{bmatrix} 0 \\ 0 \\ -\frac{1}{M} \\ \frac{1}{LM} \end{bmatrix}$$
$$C = \begin{bmatrix} 1 & 0 & 0 & 0 \\ 0 & 1 & 0 & 0 \end{bmatrix},$$

where L is the length of the pendulum's rod, an unknown parameter bounded, for this example, by $0.9\,(m) \leq L \leq 1.9\,(m)$. The parameters m and M are the mass of the small ball and the cart, respectively. It is assumed that there is a friction force (proportional to the velocity of the cart) affecting the cart and b is the friction coefficient. The following parameters are fixed and known:

$$M = 1\,(kg); \qquad m = \frac{3}{4}\,(kg); \; g = 9.8\,(m/s^2);$$
$$b = 0.1\,(kg/s); \quad k = 0.15\,(kg/s^2).$$

In addition to the uncertain length of pendulum, we also assume that there is, in the control channel, an unmodelled

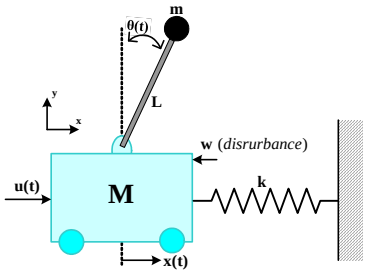

Fig. 2. Inverted Pendulum test-bed example. M, m and k are known but L is uncertain

time-delay τ whose maximum possible value is 20 ms. The frequency-domain upper-bound for the unmodelled time-delay, which serves in this example as a surrogate for unmodelled dynamics, is the frequency-domain magnitude of the first-order transfer function

$$W_{un}(s) = \frac{2.1s}{s + 50}$$

A robust H_∞ controller which stabilizes the inverted pendulum for the whole parametric uncertainty interval and unmodelled dynamics is used to regulate the cart position while the pendulum is vertically stabilized (see [13] for more details). The disturbance force $w(t)$ is a stationary first-order (coloured) stochastic process generated by driving a low-pass filter, $\frac{1}{s+1}$, with continuous-time white noise of zero mean and unit intensity.

In order to analyze the situation when the nominal values L_i, for $i = 1 \dots 4$ do not include the true parameter L, we start by recalling the concept of Equivalently Identified Plant (EIP) sets introduced for the first time in [8] [3]. As Theorem 1 shows, as long as the distinguishability condition holds, one of the dynamic weights p_i governed by (6), say $p_{i^\star}$, converges to 1 and the rest converge to 0. In this case, the actual parameter is identified as $L_{i^\star}$. It is however important to notice that it cannot be concluded that the true value of L is actually $L_{i^\star}$. However, in a well defined sense it can be said that the true values of L is closer to $L_{i^\star}$ than to any other L_i for $i \in \mathcal{I}$. This simple reasoning allows us to conclude that, corresponding to each L_i; $i = 1 \dots 4$ there is a set of plants that is naturally identified as L_i. In [8] each of these sets is called as a set of Equivalently Identified Plants (EIP), denoted by S^i_{EIP}. Corollary 1 provides a method to compute the EIP set for each L_i.

In the inverted pendulum example, we divided uniformly the interval where L can live into 4 sub-intervals. Using the results in Corollary 1, we computed the nominal values for L such that the EIP set of each observer corresponds to the sub-intervals and the following set $\kappa = \{1.025, 1.287, 1.526, 1.778\}$ was obtained for nominal values. Fig. 3 illustrates graphically how the EIP sets can be obtained and how unmodelled dynamics impacts the EIP sets. The y-axis corresponds to the deterministic norm defined in (21) between the nominal observers and the true plant, parameterized by L in $[0.9\,,\,1.9]$. The intersections of these curves define the boundaries of the EIP sets. A systematic methodology to compute the EIP sets is presented in [8]. As described in [8], unmodelled dynamics impacts upon model identification and EIP sets. The unmodelled dynamics lead to "undecidable sets" in the uncertain parameter space. If the true parameter lies in one of these sets, then one cannot guarantee which model will be selected. As mentioned before it is assumed that control force, in the inverted pendulum plant, is provided through a time-delay τ whose maximum possible value is 20 ms and this time delay can be viewed as unmodelled dynamic. Fig. 3 illustrates graphically the impact of unmodelled dynamics on the EIP sets.

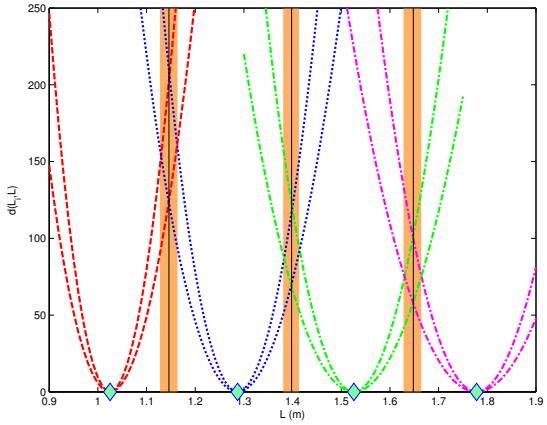

Fig. 3. Effect of Unstructured Uncertainty on Equivalently Identified Plant (EIP) Sets.

All the numerical results in this paper are the average of 5 Monte Carlo simulations. A 2 ms time delay in the controller channel was set. We have used different values of the pendulum length (as the constant unknown parameters) in the simulations and except for the values which are very close to the boundaries, the correct model is always identified (the results are not shown due to the space limitations). We stress that the performance of any adaptive system must be evaluated not only for constant unknown parameters but also, for time-varying parameters which undergo slow or rapid time-variations. In what follows we examine different scenarios where the unknown parameter, L, changes fast or slowly.

Case I: Length L changing slowly

We start by analyzing the behavior of the CT-MMAE under the pendulum length time-variation shown in the first subplot of Fig. 4. The pendulum length is steady for 5 s. Then, it changes linearly until it is within the next model, keeping steady for another 5 s, and repeating the procedure. These changes take 5 s each, so the slope is, in general, not always the same. This is shown in the first subplot of the Fig. 4, which also shows (using the dashed lines) the model boundaries as defined by Fig. 3. The time evolution of the dynamic weights are also shown in Fig. 4. Note that the dynamic weights respond very fast to the model changes. Fig. 5 displays the time evolution of the output (x and θ), the estimated output ($\hat{x}$ and $\hat{\theta}$), and the output estimation errors. The right column is a zoom in on these signals over a smaller time-window. The Mont-Carlo simulation results

[3]The concept of EIP sets and the impact of unmodelled dynamics on the EIP sets described in [8] for the discrete-time MMAE can be easily extended to the continuous-time case.

show that the true model is always correctly identified even when L is near the boundary between two adjacent EIP sets.

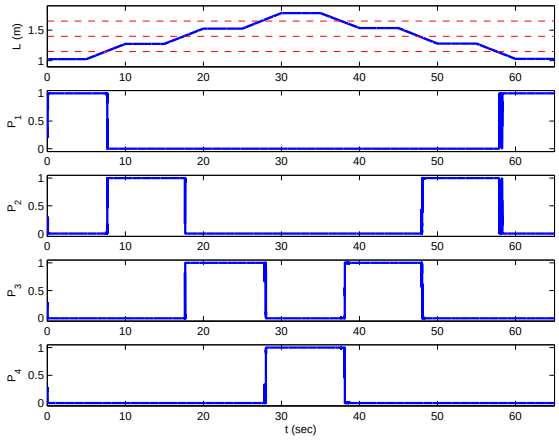

Fig. 4. Dynamic weights while L varies in the time.

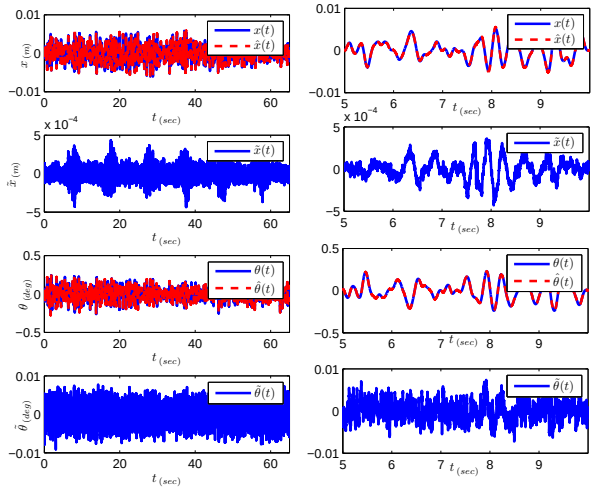

Fig. 5. Output Estimations and Residuals.

Case II: Length L with step changes

Next, a slightly different scenario is analyzed. The pendulum length time variation is the staircase function shown in the first subplot of Fig. 6, which means that it stays constant for 5 s and then jumps to another constant value. The dynamic weights evolution are shown in Fig. 6.

V. Conclusion and Future Works

We presented and analyzed a class of CT-MMAE systems for MIMO continuous-time systems with parametric uncertainty. We developed a distance-like pseudo norm between the true plant and the identified model in a deterministic setting, based on the energy of the output error signals. We showed that if a certain distinguishability condition holds, then the model that is identified is the one closest to the true plant in a well defined norm sense. In particular, with an illustrative example, we revisited the concept of undecidable sets (introduced in [8]), which capture the fact that unmodelled uncertainty will necessarily lead to basic limitations to identification. This issue and that of determining general

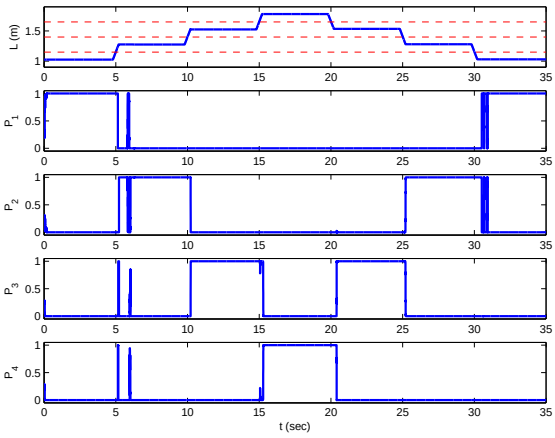

Fig. 6. Dynamic weights while L varies in the time.

geometric properties of the EIP sets deserve further research. Another topic that warrants consideration is that of deriving adaptive control systems for uncertain plants (especially unstable and non-minimum phase plants) using the multiple model approach.

VI. Acknowledgments

We thank our colleagues Paulo Rosa and J. Vasconcelos for many discussions on adaptive estimation.

References

[1] D. T. Magill, "Optimal adaptive estimation of sampled stochastic processes," *IEEE Trans. on Automat. Contr.*, vol. 10, pp. 434–439, 1965.

[2] B. D. O. Anderson and J. B. Moore, *Optimal Filtering*. New Jersey, USA: Prentice-Hall, 1979.

[3] Y. Baram and N. Sandell, "An information theoretic approach to dynamical systems modeling and identification," *IEEE Trans. on Automat. Contr.*, vol. 23, pp. 61–66, 1978.

[4] X. R. Li and Y. Bar-Shalom, "Multiple-model estimation with variable structure," *IEEE Trans. on Automat. Contr.*, vol. 41, pp. 478–493, 1996.

[5] W. S. Chaer, R. H. Bishop, and J. Ghosh, "A mixture-of-experts framework for adaptive kalman filtering," *IEEE Transactions on System, Man, and Cybernetic- Part B: Cybernetic*, vol. 27, pp. 452–464, 1997.

[6] A. P. Aguiar, M. Athans, and A. Pascoal, "Convergence properties of a continuous-time multiple-model adaptive estimator," in *Proc. of ECC'07 - European Control Conference*, Kos, Greece, Jul. 2007.

[7] A. P. Aguiar, V. Hassani, A. M. Pascoal, and M. Athans, "Identifcation and convergence analysis of a class of continuous-time multiple-model adaptive estimators," in *Proc. of the 17th IFAC World Congress*, Seoul, Korea, Jul. 2008.

[8] V. Hassani, A. P. Aguiar, M. Athans, and A. M. Pascoal, "Multiple model adaptive estimation and model identification using a minimum energy criterion," in *Proc. of ACC'09 - American Control Conference*, St. Louis, Missouri, USA, 2009.

[9] K.-P. Dunn and I. B. Rhodes, "A generalized representation theorem with applications to estimation and hypothesis testing," in *Proc of the 11th Annual Allerton Conf. on Circuit and System Theory*, 1973.

[10] K.-P. Dunn, "Measure transformation, estimation, detection and stochastic control," Ph.D. dissertation, Washington University, St. Louis, MO, USA, 1974.

[11] A. Krener, "Kalman-Bucy and minimax filtering," *IEEE Trans. on Automat. Contr.*, vol. 25, pp. 291–292, 1980.

[12] V. Hassani, A. P. Aguiar, A. M. Pascoal, and M. Athans, "Further results on plant parameter identification using continuous-time multiple-model adaptive estimators," Institute for Systems and Robotics (ISR), Instituto Superior Técnico (IST), Lisbon, Portugal, Tech. Rep. ISR-IST-UTL-09-03, 2009.

[13] V. Hassani, M. Athans, and A. M. Pascoal, "An application of the RMMAC methodology to an unstable plant," in *Proc. of MED'09 - The 17th Mediterranean Conference on Control and Automation*, Thessaloniki, Greece, 2009.